

Nonlinear elastic deformation of Mindlin torus

B. H. Sun^{a,1}

^a*School of Civil Engineering & Institute of Mechanics and Technology, Xi'an University of Architecture and Technology, Xi'an 710055, China*

ARTICLE INFO

Keywords:

circular torus, nonlinear deformation, shear deformation, Mindlin, Gauss curvature, Maple

ABSTRACT


The nonlinear deformation and stress analysis of a circular torus is a difficult undertaking due to its complicated topology and the variation of the Gauss curvature. A nonlinear deformation (only one term in strain is omitted) of Mindlin torus was formulated in terms of the generalized displacement, and a general Maple code was written for numerical simulations. Numerical investigations show that the results obtained by nonlinear Mindlin, linear Mindlin, nonlinear Kirchhoff-Love, and linear Kirchhoff-Love models are close to each other. The study further reveals that the linear Kirchhoff-Love modeling of the circular torus gives good accuracy and provides assurance that the nonlinear deformation and stress analysis (not dynamics) of a Mindlin torus can be replaced by a simpler formulation, such as a linear Kirchhoff-Love theory of the torus, which has not been reported in the literature.


1. Introduction

Torii or toroidal shells are widely used in various industrial applications, such as water tanks, fuel reactor shells, rocket fuel tanks, and piping. The torus has been studied for more than 110 years. For a review on the analysis of axisymmetric toroidal shells, including a historical perspective, the reader is referred to the literature [1, 2, 3, 4, 5, 6, 7, 9, 10, 11, 12].

Reissner [13] and Meissner [14, 15] derived a mixed equation to determine the elastic deformation of shells of revolution under axisymmetric loading [5]. Wissler [16] applied the Reissner-Meissner equations to toroidal shells and obtained the first exact series solutions. Tölke [17] further expanded the Reissner-Meissner theory, combining the equations by cleverly transforming them into a single complex differential equation. Tölke's complex differential formulation was later fur-

*Corresponding author.

 sunbohua@xauat.edu.cn (B.H. Sun)

 imt.xauat.edu.cn (B.H. Sun); +8615001102877 (B.H. Sun)

ther developed into a general theory of shells by Novozhilov [1]. Chang (name later changed to Zhang) [18] proposed an asymptotic solution of Tölke's toroidal equations in the $1/3$ -order Bessel functions and search of his group [19]. Tao [20] obtained the exact homogenous solution of the Reissner-Meissner torus equation in terms of the Heun function [21]. Sun [10, 11] obtained the exact solution of the Novozhilov torus equation in terms of Heun functions as well, and proposed a computational algorithm based on the Novozhilov equation [1]. Sun [11] studied the geometry-induced rigidity in an elastic torus from a circular to oblique elliptic cross-section based on the nonlinear Kirchhoff-Love theory of shells.

In classical plate/shell theory [28], the transverse normal and shear stresses are neglected. The first-order shear deformation plate/shell theory extends the kinematics of the classical shell theory (CST) by relaxing the normal restrictions and allowing for arbitrary but constant rotation of transverse normals [22, 23, 24]. The third-order shear deformation plate/shell theory further relaxes the kinematics hypothesis by removing the straightness assumptions, i.e., the straight normal to the middle surface before deformation may become cubic curves after deformation [25]. The most significant difference between the classical and shear deformation theories is the effect of including transverse shear deformation on the predicted deflections, buckling loads, and frequencies. In general, the classical plate/shell theory under-predicts deflection and over-predicts frequency as well as buckling loads of plates/shells with a side-to-thickness ratio of order 20. Therefore, for a thick shell with a side-to-thickness ratio of order less than 20, the first- or third-order shear deformation shell theory should be used [26]. The reason behind the difference is that the shells with the classical kinematics are "stiffer" than those with the higher-order kinematics. Regarding the nonlinear shear deformation of the torus, or the so-called Mindlin torus, no results have been reported in the literature, except [27], in which the natural frequencies of moderately thick and thick toroidal shells were studied.

To investigate the influence of the shear deformation on the torus, the Mindlin displacement model is applied to the torus in this work. The rest of this paper is organized as follows. In Section 2, the nonlinear displacement governing equations of the Mindlin torus are derived. Several numerical investigations on the circular Mindlin torus acted on by internal pressure and combined forces are carried out in Sections 3 and 4. Results from different models of the theory of shells are presented in Section 5. Conclusions with perspectives are given in Section 6.

2. Formulation of elastic Mindlin torus in terms of generalized displacement field

Up to now, there have been three kind of formulations of a torus, i.e., the mixed formulation [13, 15], complex-form formulation [1, 17], and displacement formulation [11]. Each has different advantage and disadvantages, and the governing equations in terms of displacement must be adopted for nonlinear shear deformation of shells.

Recently, [11] derived the displacement equations of the torus using the Kirchhoff-Love theory, which assumes that a normal line remains straight and perpendicular to the neutral plane of the shell middle surface during bending. In contrast, Mindlin theory retains the assumption that the line remains straight, but is no longer perpendicular to the neutral plane. This means that Kirchhoff theory applies to thin plates, while Mindlin theory applies to thick plates, in which shear deformation may be significant.

A surface of revolution is generated by the rotation of a plane curve about an axis in its plane. This generating curve is called a meridian, and an arbitrary point on the middle surface of the shell is described by specifying the particular meridian on which it is found, and by giving the value of a second coordinate that varies along the meridian and is constant on a circle around the axis of the shell, which is called a latitude circle [5].

A meridian is identified by the angular distance θ of its plane from that of a datum meridian and a second coordinate is chosen, namely, the angle ϕ between a normal to the shell and its axis

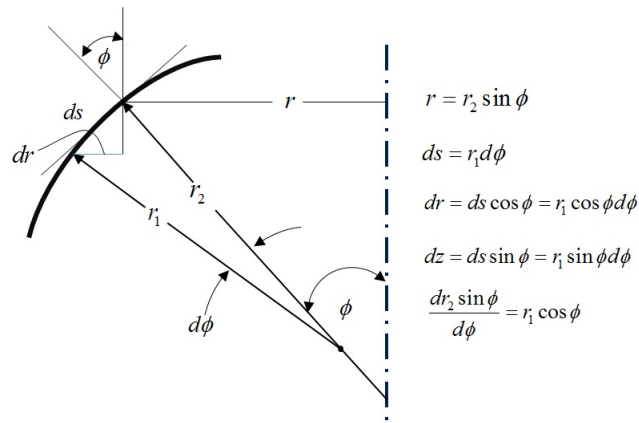


Figure 1: Surface of revolution.

of revolution. If the middle surface of the shell is a sphere, these coordinates are the spherical coordinates used in geography: θ is the longitude and ϕ is the complement to the latitude, i.e., the co-latitude [5].

Figure 1 shows a meridian of the shell. Let r be the distance of one of its points from the axis of rotation and r_1 its radius of curvature. In our equations we also need the length r_2 , measured on a normal to the meridian between its intersection with the axis of rotation and the middle surface. It is the second radius of curvature of the shell, and we read from Fig. 1 the relation $r = r_2 \sin \phi$. For the line element ds of the meridian, we have $ds = r_1 d\phi$, and since $dr = ds \cos \phi$ and $dz = ds \sin \phi$, we have the relations $\frac{dr}{d\phi} = r_1 \cos \phi$, $\frac{dz}{d\phi} = r_1 \sin \phi$ and Gauss-Codazzi relation $\frac{dr_2 \sin \phi}{d\phi} = r_1 \cos \phi$.

For the shells of revolution shown in Fig. 1, the positions of points on the middle surface will be determined by the angles θ and ϕ . Further, let r_1 be the radius of curvature of the meridian and r_2 the radius of curvature of the normal section, tangential to the parallel circle. This second radius is equal to the segment of the perpendicular to the middle surface between this surface and the axis of the torus.

The principal radii r_2 are given by $r_2 = \frac{x}{\sin \phi} = \frac{R+a \sin \phi}{\sin \phi}$. Applying the Gauss-Codazzi relation $r_1 \cos \phi = \frac{dr_2 \sin \phi}{d\phi}$, we find principal radii $r_1 = \frac{1}{\cos \phi} \frac{dr_2 \sin \phi}{d\phi}$. Therefore, we have the principal radii of the circular torus as follows: $r_1 = a$, $r_2 = \frac{R}{\sin \phi} + a$.

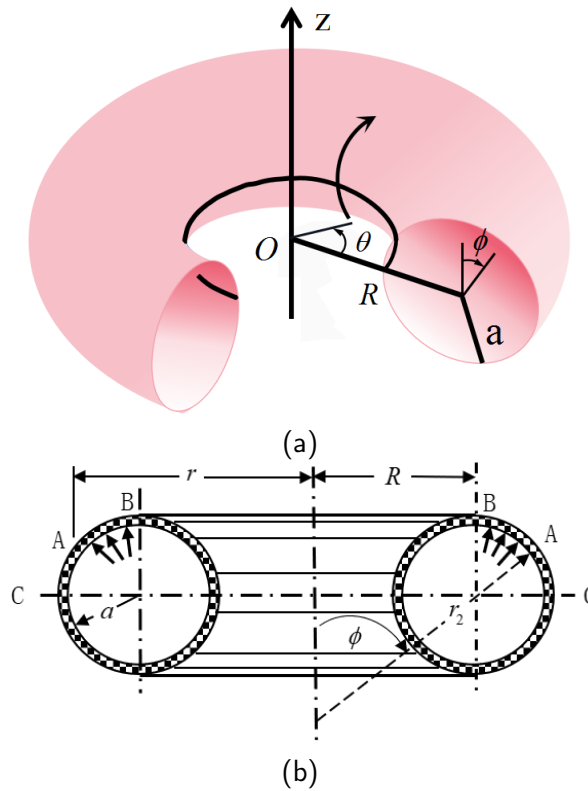


Figure 2: Geometry of the torus; the Lamé coefficients are $A_1 = r_1$, and $A_2 = r_2 \sin \phi$

Under the same assumptions and restrictions as in the classical plate theory, but relaxing the normality conditions, for the first-order theory, the displacement field (U, V, W) in a shell can be expressed in the form

$$U(\phi, \theta) = u(\phi) + \zeta \vartheta(\phi),$$

$$V(\phi, \theta) = 0, \tag{1}$$

$$W(\phi, \theta) = w(\phi),$$

in which ξ is coordinate in thickness direction, (u, v, w) are the displacements on the mid-surface of the shell and (ϑ) are the rotations of a normal to the reference surface. (u, w, ϑ) are the generalized displacements of the torus.

The strain and curvature change of the full nonlinear theory of shells [6, 26, 28, 29] are shown

Table 1Full nonlinear theory: strain field (ϵ_ϕ , ϵ_θ), the change of curvature (κ_ϕ , κ_θ)and the shear strain γ_ϕ

| | | |
|-------------------|---|--|
| ϵ_ϕ | = | $\frac{1}{a}(\frac{du}{d\phi} + w) + \frac{1}{2} \frac{1}{a^2} (\frac{du}{d\phi} + w)^2 + \frac{1}{2} \vartheta^2$ |
| ϵ_θ | = | $\frac{\sin \phi}{R+a \sin \phi} (u \cot \phi + w) + \frac{1}{2} \left[\frac{\sin \phi}{R+a \sin \phi} (u \cot \phi + w) \right]^2$ |
| κ_ϕ | = | $\frac{1}{a} \frac{d\vartheta}{d\phi} + \frac{1}{a} (\frac{du}{d\phi} + w) \frac{1}{a} \frac{d\vartheta}{d\phi} + \frac{1}{a^2} \vartheta^2$ |
| κ_θ | = | $\frac{\cos \phi}{R+a \sin \phi} \vartheta + \frac{\sin \phi \cos \phi}{(R+a \sin \phi)^2} \vartheta (u \cot \phi + w)$ |
| γ_ϕ | = | $\vartheta + \frac{1}{a} \frac{dw}{d\phi} - \frac{u}{a}$ |

Table 2Shallow shells: the strain field (ϵ_ϕ , ϵ_θ) and the change of curvature (κ_ϕ , κ_θ) and the shear strain γ_ϕ

| | | |
|-------------------|---|---|
| ϵ_ϕ | = | $\frac{1}{a}(\frac{du}{d\phi} + w) + \frac{1}{2} \vartheta^2$ |
| ϵ_θ | = | $\frac{\sin \phi}{R+a \sin \phi} (u \cot \phi + w)$ |
| κ_ϕ | = | $\frac{1}{a} \frac{d\vartheta}{d\phi}$ |
| κ_θ | = | $\frac{\cos \phi}{R+a \sin \phi} \vartheta$ |
| γ_ϕ | = | $\vartheta + \frac{1}{a} \frac{dw}{d\phi} - \frac{u}{a}$ |

in Table 1.

Based on the above full strain field, several approximations are proposed [6, 26, 28, 29]. A popular one is the nonlinear theory of shallow shells [26], which can be formulated by omitting all the underbrace terms in Table 1; the strain fields of the theory of shallow shells are shown in Table 2.

It should be noted that if the term, $\frac{1}{2} \frac{1}{a^2} (\frac{du}{d\phi} + w)^2$, were kept, the Maple code in the appendix does not work due to the fact that the dsolve/numeric/bvp/convertsys unable to convert to an explicit first-order system. In order to find out which term causes the problem, let's check the structure of

Table 3

A nonlinear theory: strain field $(\varepsilon_\phi, \varepsilon_\theta)$, the change of curvature $(\kappa_\phi, \kappa_\theta)$ and the shear strain γ_ϕ to be used in this paper

| | | |
|----------------------|---|--|
| ε_ϕ | = | $\frac{1}{a}(\frac{du}{d\phi} + w) + \frac{1}{2} \frac{1}{a^2} (w \frac{du}{d\phi} + w^2) + \frac{1}{2} \vartheta^2$ |
| ε_θ | = | $\frac{\sin \phi}{R+a \sin \phi} (u \cot \phi + w) + \frac{1}{2} [\frac{\sin \phi}{R+a \sin \phi} (u \cot \phi + w)]^2$ |
| κ_ϕ | = | $\frac{1}{a} \frac{d\vartheta}{d\phi} + \frac{1}{a} (\frac{du}{d\phi} + w) \frac{1}{a} \frac{d\vartheta}{d\phi} + \frac{1}{a^2} \vartheta^2$ |
| κ_θ | = | $\frac{\cos \phi}{R+a \sin \phi} \vartheta + \frac{\sin \phi \cos \phi}{(R+a \sin \phi)^2} \vartheta (u \cot \phi + w)$ |
| γ_ϕ | = | $\vartheta + \frac{1}{a} \frac{dw}{d\phi} - \frac{u}{a}$ |

the term $\frac{1}{2} \frac{1}{a^2} (\frac{du}{d\phi} + w)^2$, which can be expanded as follows

$$\frac{1}{2} \frac{1}{a^2} (\frac{du}{d\phi} + w)^2 = \frac{1}{2} \frac{1}{a^2} [\underbrace{(\frac{du}{d\phi})^2}_{\text{underbrace}} + w \frac{du}{d\phi} + w^2]. \quad (2)$$

After trying, we found that the underbrace term, $(\frac{du}{d\phi})^2$, is the source of the problem, which will be delectable compared with other terms, because the deformation in the meridian direction ϕ is relatively smaller than the deformation in the hoop or angular θ direction.

To capture more rich deformation information, the strain field $(\varepsilon_\phi, \varepsilon_\theta)$, the change of curvature $(\kappa_\phi, \kappa_\theta)$ and shear strain (γ_ϕ) are used in this paper, as shown in Table 3.

It worth mentioning that a circular torus using the nonlinear strain field listed in Table 3 has not been seen in the literature.

The resultant membrane forces are $N_\phi = K(\varepsilon_\phi + \nu \varepsilon_\theta)$, $N_\theta = K(\nu \varepsilon_\phi + \varepsilon_\theta)$, the resultant bending moments are $M_\phi = B(\kappa_\phi + \nu \kappa_\theta)$, $M_\theta = B(\nu \kappa_\phi + \kappa_\theta)$, and resultant shear force $Q_\phi = \kappa G h \gamma_\phi$, where the membrane stiffness $K = \frac{Eh}{1-\nu^2}$, the bending stiffness $B = \frac{Eh^3}{12(1-\nu^2)}$, the thickness is denoted by h , the Young's modulus is denoted by E , and the Poisson ratio is denoted by ν , and $\kappa = \frac{5}{6}$ is called shear correction factor [26].

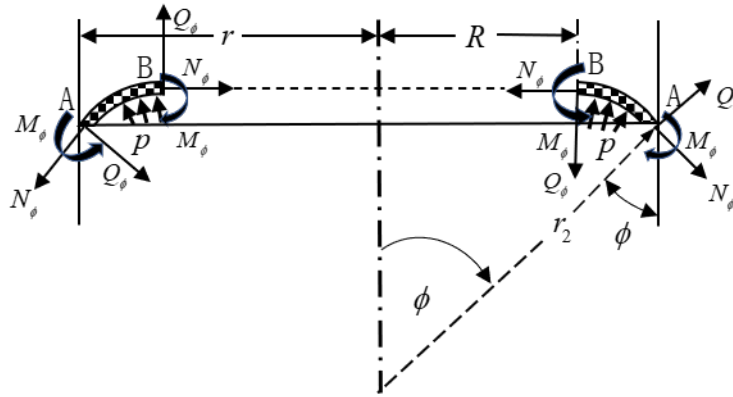


Figure 3: Loading, forces, and moments of the torus

Regarding the forces shown in Fig. 3, the balance equations [26] are

$$\begin{aligned}
 & \frac{d}{d\phi}((R + a \sin \phi)N_\phi) - aN_\theta \cos \phi + (R + a \sin \phi)Q_\phi \\
 & - (R + a \sin \phi)N_\phi \vartheta + a(R + a \sin \phi)q_\phi = 0, \\
 & \frac{d}{d\phi}((R + a \sin \phi)Q_\phi) - a(R + a \sin \phi)\left(\frac{N_\phi}{a} + \frac{N_\theta \sin \phi}{R + a \sin \phi}\right) \\
 & - \frac{d}{d\phi}((R + a \sin \phi)N_\phi \vartheta) + a(R + a \sin \phi)q_\zeta = 0, \\
 & \frac{d}{d\phi}((R + a \sin \phi)M_\phi) - a \cos \phi M_\theta - a(R + a \sin \phi)Q_\phi = 0,
 \end{aligned} \tag{3}$$

where the distributed loads q_ϕ and $q_\zeta = p$ are along the ϕ and ζ directions, respectively.

Equation 3 can be further simplified by substituting the constitutive relations into Eq. 3, which will generate final equations as a six-order nonlinear ordinary differential equation (ODE) system about the generalized displacement (u, w, ϑ) . Clearly, the ODE system has no analytical solution and we must turn to a numerical solution.

For simplification of presentation, physical units will not be plotted in all figures, and are listed in Table 4.

Table 4

Physical units used in this paper

| R | a | h | E | ν | M_ϕ | N_ϕ |
|----------|---------------|-----|---------|------------|----------|----------|
| m | m | m | N/m^2 | 1 | N | N/m |
| Q_ϕ | σ_ϕ | u | w | δ_z | | |
| N/m | N/m^2 | m | m | m | | |

Note: N is the physical unit of force and denotes Newtons.

3. Half-torus acted on by combined loads F , P , and M at free boundary

When there were no oblique angles, namely, $\beta = 0$, all formulations reduced to the normal elliptic torus. A normal torus with a cut along its parallel at $\phi = \frac{\pi}{2}$ or $\phi = -\frac{\pi}{2}$ under load F is shown in Fig. 4.

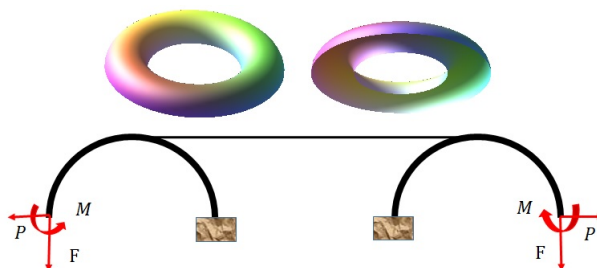


Figure 4: $u(-\frac{\pi}{2}) = 0$, $w(-\frac{\pi}{2}) = 0$, $\frac{dw}{d\phi}(-\frac{\pi}{2}) = 0$, $N_\phi(\pi) = 0$, $Q_\phi(\pi) = P$, $M_\phi(\pi) = M$

From combined results shown in Fig. 5, it is clear that the stress and deformation are affected by the thickness change.

4. A 3/2-half-torus acted on by the combined loads F , P , and M at free boundary

A $\frac{3}{2}$ -half-torus acted on by combined loads is shown in Fig. 6.

A $\frac{3}{2}$ -half-circular-torus with a fixed boundary at $\phi = -\frac{\pi}{2}$ and $\phi = \pi$ acted on by F , P , M , and q is shown in Fig. 6. For this problem, we will vary the thickness while keeping other parameters constant. The numerical results of the circular torus are shown in Fig. 7.

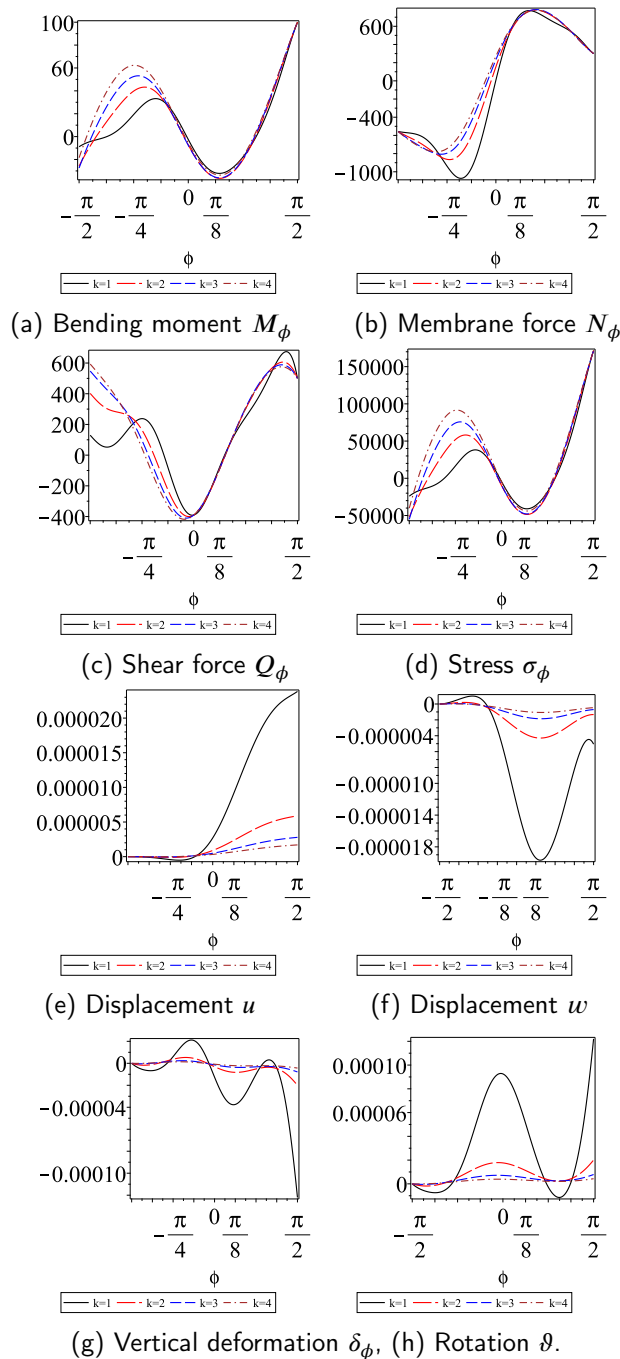


Figure 5: Torus under the combined loads F , P , and M . Torus data: $a = 0.3[m]$, $R = 1[m]$, $E = 2.0 \times 10^{11} N/m^2$, $\nu = 0.3$, $M = 100[N]$, $F = 300[N/m]$, $P = 500[N/m]$, and $h = 0.05k[m]$

5. Comparison of studies and discussion: Mindlin torus vs. Kirchhoff-Love torus

To show the effect of the shear deformation on the strength and deformation of the torus and validation of the Kirchhoff-Love assumption, we present some comparison studies between the

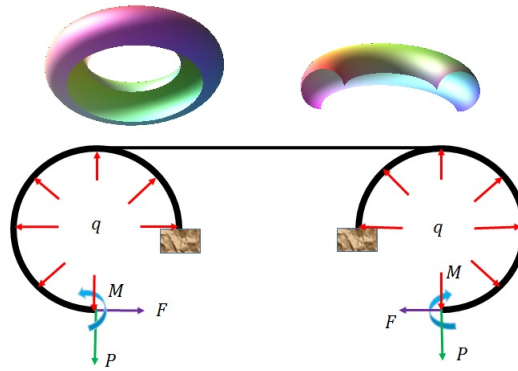


Figure 6: $u(-\frac{\pi}{2}) = 0$, $w(-\frac{\pi}{2}) = 0$, $\frac{dw}{d\phi}(-\frac{\pi}{2}) = 0$, $N_\phi(\pi) = 0$, $Q_\phi(\pi) = P$, $M_\phi(\pi) = M$

Table 5

Full nonlinear Kirchhoff-Love theory: strain field $(\epsilon_\phi, \epsilon_\theta)$ and the change of curvature $(\kappa_\phi, \kappa_\theta)$

| | | |
|-------------------|---|---|
| ϵ_ϕ | = | $\frac{1}{a}(\frac{du}{d\phi} + w) + \frac{1}{2}(-\frac{1}{a}\frac{dw}{d\phi} + \frac{u}{a})^2$, |
| ϵ_θ | = | $\frac{\sin\phi}{R+a\sin\phi}(u\cot\phi + w) + \frac{1}{2}[\frac{\sin\phi}{R+a\sin\phi}(u\cot\phi + w)]^2$ |
| κ_ϕ | = | $\frac{1}{a}\frac{d}{d\phi}(-\frac{1}{a}\frac{dw}{d\phi} + \frac{u}{a}) + \frac{1}{a^2}(\frac{du}{d\phi} + w)\frac{d}{d\phi}(-\frac{1}{a}\frac{dw}{d\phi} + \frac{u}{a}) + \frac{1}{a^2}(-\frac{1}{a}\frac{dw}{d\phi} + \frac{u}{a})^2$, |
| κ_θ | = | $\frac{\cos\phi}{R+a\sin\phi}(-\frac{1}{a}\frac{dw}{d\phi} + \frac{u}{a}) + \frac{\sin\phi\cos\phi}{(R+a\sin\phi)^2}(-\frac{1}{a}\frac{dw}{d\phi} + \frac{u}{a})(u\cot\phi + w)$ |

Mindlin torus and Kirchhoff-Love torus in both nonlinear and linear deformations.

For comparison purpose, the strain field of the Kirchhoff-Love shells can be obtained by replacing the rotation ϑ by $\vartheta = -\frac{1}{a}\frac{dw}{d\phi} + \frac{u}{a}$, and then we have the strain field of the Kirchhoff-Love shells as shown in Table 5.

In the following, we will test both Mindlin and Kirchhoff-Love assumptions for thick shells, for which the thickness is $h < \frac{a}{5}$, which is beyond the range of the thin-shell assumption $h < \frac{a}{20}$. As previously, we only change the torus thickness while keeping all other parameters constant. The comparisons are shown in Fig. 8.

The digital results of the internal moment and force are listed in Table 6. Some abbreviations are defined as: NLinM, nonlinear Mindlin; LinM, linear Mindlin; NlinKL, nonlinear Kirchhoff-Love; LinKL, Kirchhoff-Love.

The numerical studies show that the results of NLinM are close to those of LinM, NLinKL, and LinKL, except for the shear force Q_ϕ .

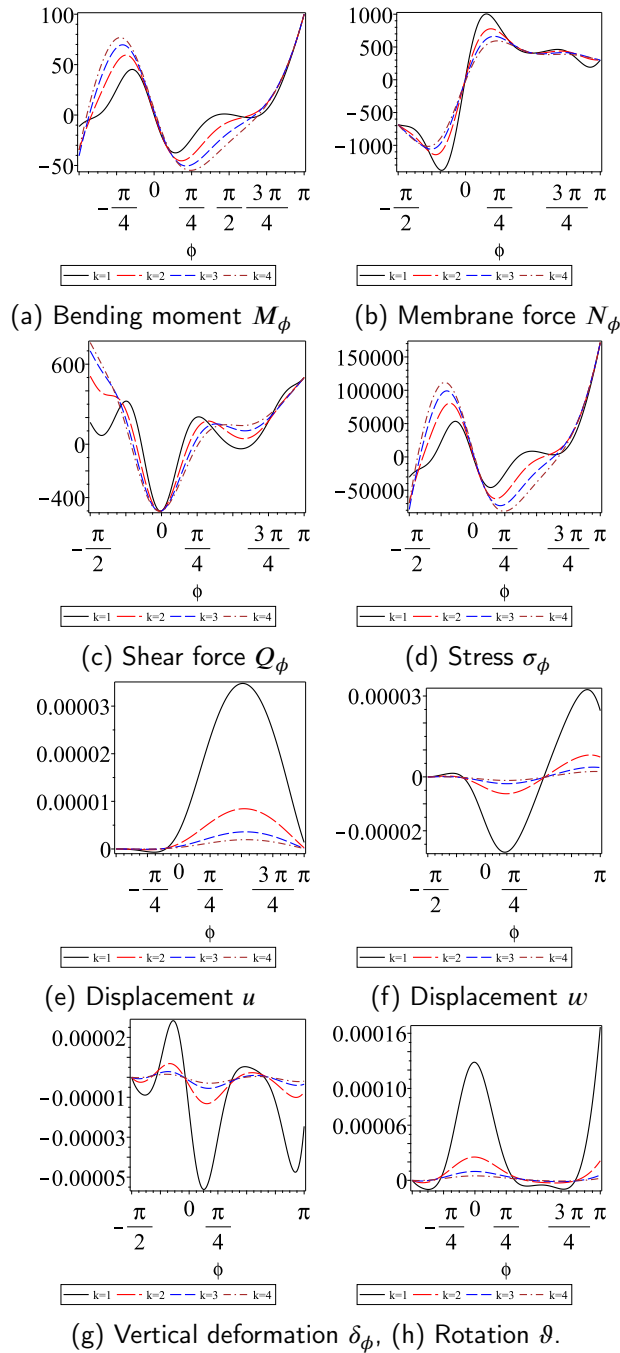


Figure 7: Torus data: $a = 0.3[m]$, $R = 1[m]$, $h = \frac{a}{10}[m]$, $E = 2.0 \times 10^{11} N/m^2$, $\nu = 0.3$, $q = 80[N/m^2]$, $F = 300[N/m]$, $P = 500[N/m]$, $M = 100[N]$

The digital results of the generalized displacement (u , w , ϑ) are listed in Table 7.

The numerical studies show that the generalized displacements (u , w , ϑ) of NLinM are close to those of LinM, NLinKL, and LinKL in the case of thickness $h = 4h_{\text{thin}}$, where the thickness of a

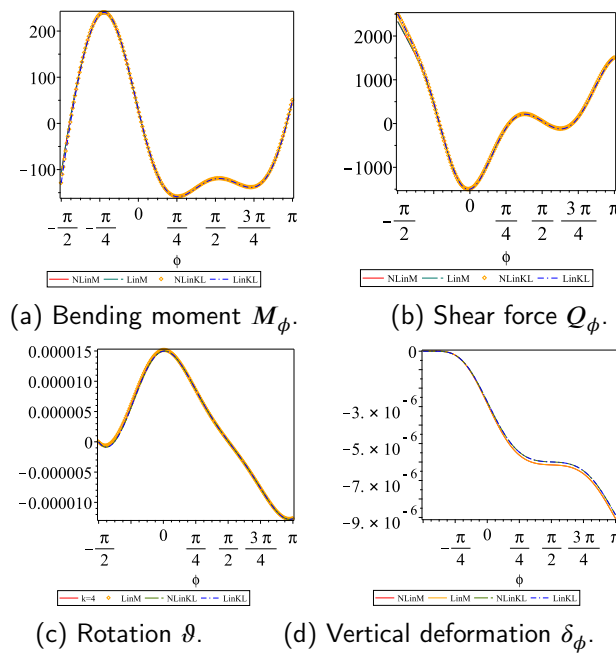


Figure 8: Torus data: $a = 0.3[m]$, $R = 1[m]$, $E = 2.0 \times 10^{11} N/m^2$, $\nu = 0.3$, $q = 20[N/m^2]$, $F = 200[N/m]$, $P = 1500[N/m]$, $M = 50[N]$ and $h = \frac{a}{5} = 0.06[m]$

Table 6

Results of moment and membrane force

| $(\phi = -\frac{\pi}{2})$ | NLinM | LinM | NLinKL | LinKL |
|---------------------------|-----------|-----------|-----------|-----------|
| $M_\phi[N]$ | -107.983 | -107.982 | -129.328 | -129.327 |
| $N_\phi[N/m]$ | -2135.575 | -2135.571 | -2135.575 | -2135.571 |
| $Q_\phi[N/m]$ | 2331.061 | 2331.036 | 2505.783 | 2505.756 |

NLinM, nonlinear Mindlin; LinM, linear Mindlin; NlinKL, nonlinear Kirchhoff-Love; LinKL, Kirchhoff-Love

Table 7

Generalized displacement (u , w , ϑ)

| $(\phi = \pi)$ | NLinM | LinM | NLinKL | LinKL |
|----------------|-------------|-------------|-------------|-------------|
| $u[m]$ | $-7.228e-7$ | $-7.228e-7$ | $-7.157e-7$ | $-7.157e-7$ |
| $w[m]$ | $9.062e-6$ | $9.062e-6$ | $8.860e-6$ | $8.860e-6$ |
| ϑ | $-0.127e-4$ | $-0.127e-4$ | $-0.127e-4$ | $-0.127e-4$ |

NLinM, nonlinear Mindlin; LinM, linear Mindlin; NlinKL, nonlinear Kirchhoff-Love; LinKL, Kirchhoff-Love

thin torus is defined as $h_{\text{thin}} = \frac{a}{20}$. The torus with thickness h can be definitely considered a "thick" torus.

The comparison studies clearly indicate that the nonlinear Mindlin torus modeling can be replaced by the modeling of the linear Kirchhoff-Love torus. The reason behind this scenario is that

all the square terms of both strain and rotation can be neglected from elastic energy perspectives.

To have a better idea on the contribution of different energy densities, the shearing energy density, bending energy density and membrane energy density are shown in Fig.9. The numerical results of the elastic energy densities have not been seen in the literature.

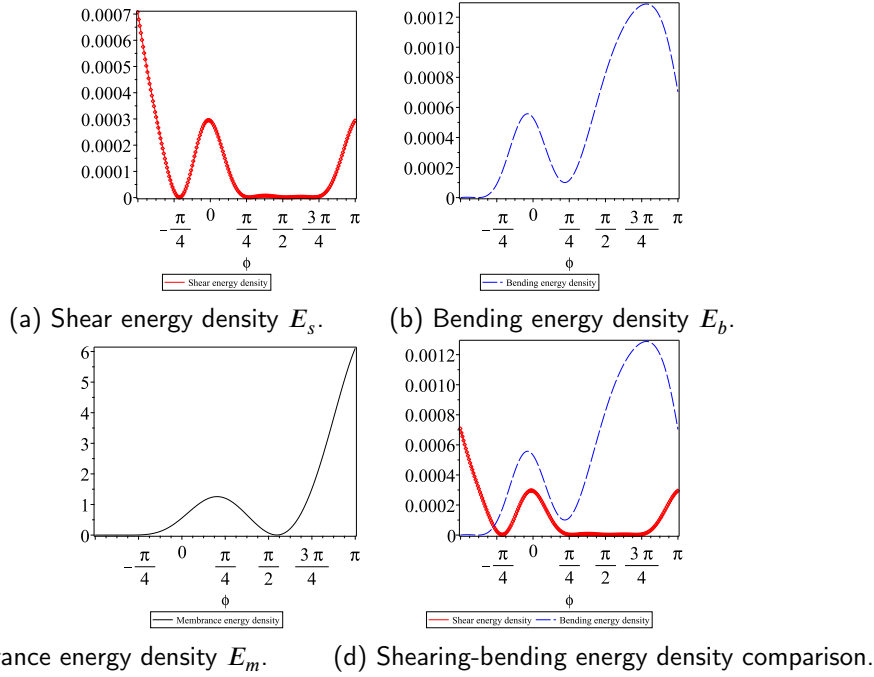


Figure 9: Torus data: $a = 0.3[m]$, $R = 1[m]$, $E = 2.0 \times 10^{11} N/m^2$, $\nu = 0.3$, $q = 20[N/m^2]$, $F = 200[N/m]$, $P = 1500[N/m]$, $M = 50[N]$ and $h = \frac{a}{5} = 0.06[m]$

Fig.9 clearly reveals that the bending energy is bigger than the shear energy, and membrane energy is much bigger than both bending energy and shear energy. Therefore, the shearing energy makes little contribution to the deformation and stress of the circular torus and can be omitted, namely

$$E = E_m + E_b + E_s \approx E_m + E_b, \quad (4)$$

where the total elastic energy density E , the membrane energy density $E_m = \frac{1}{2}(N_\phi \epsilon_\phi + N_\theta \epsilon_\theta)$, the bending energy density $E_b = \frac{1}{2}(M_\phi \kappa_\phi + M_\theta \kappa_\theta)$, and shear energy density $E_s = \frac{1}{2}Q_\phi \gamma_\phi$.

The above statement can not be applied to the high frequency dynamics of Mindlin torus, because for dynamics the shearing effect will be enormous and can't be omitted anymore [22, 23, 24, 31, 32].

6. Conclusions

The full nonlinear displacement formulations were derived for the Mindlin torus. To verify the formulation, we wrote a Maple code and carried out several numerical simulations. Our investigations show that the results obtained by the nonlinear Mindlin, linear Mindlin, nonlinear Kirchhoff-Love, and linear Kirchhoff-Love models are close to each other due to the domination of combining effect of membrane and bending deformation. The study reveals that the linear Kirchhoff-Love modeling of the circular torus gives good accuracy, the nonlinear deformation analysis of a Mindlin torus can be simply replaced by a simpler formulation, such as the linear Kirchhoff-Love theory of a torus, which is a remarkable result.

Acknowledgments:

I thank my students, as follows: Mr. Yong Sun for the preparation of Fig. 1, Mr. Xiong Li for the preparation of Fig. 2 (a), and Mr. Jie Wei for the preparation of Figs. 2(b) and 3. I also wish to express my deep gratitude to Prof. J.S. Yang from University Nebraska for the discussion on the origin of Mindlin's theory for the high frequency vibrations of crystal plates.

Data availability:

The data that support the findings of this study are available from the author.

Appendix: Maple code of full nonlinear theory of circular torus

Note: The code is written using Maple solver rkf45, which finds a numerical solution using a Fehlberg fourth-/fifth-order Runge-Kutta method with degree-four interpolation.

```
restart; with(plots); Digits := 20;
```

```

for k from 2 to 4 do
a := 0.3;b := a;R := 1;h := a/20*k;
mu := 0.3;E := 2*10e+11;
K := E*h/(-mu*mu + 1);B := E*h*h*h/(12*(-mu*mu + 1));
kappa := 5/6;G := E/(2*(1 + mu));
q1:= 0;qn := 20;
F := 200;P := 1500;m := 50;
R1 := a;R2 := a + R/sin(phi);
A1 := R1;A2 := R2*sin(phi);
e11 := diff(u(phi), phi)/A1 + w(phi)/R1;
e12 := 0;e13 := -vartheta(phi);
e22 := diff(A2, phi)*u(phi)/(A1*A2) + w(phi)/R2;
e21 := 0; e23 := 0;
varepsilon1 := e11 + diff(u(phi), phi)*w(phi)/(A1*R1)
+ 1/2*w(phi)/R1*w(phi)/R1 + e13*e13/2
varepsilon2 := e22 + 1/2*e22*e22;
k11 := diff(vartheta(phi), phi)/A1;
k12 := 0; k13 := -vartheta(phi)/R1;
k22 := diff(A2, phi)*vartheta(phi)/(A1*A2);
k21 := 0;k23 := 0;
varkappa1 := e11*k11 + e12*k12 + e13*k13 + k11;
varkappa2 := e21*k21 + e22*k22 + e23*k23 + k22;
T2 := K*(mu*varepsilon1 + varepsilon2);
M2 := B*(mu*varkappa1 + varkappa2);

```



```

N1 := kappa*G*h*(vartheta(phi) + diff(w(phi), phi)/A1 - u(phi)/R1);
sun1 := T1(phi) = K*(mu*varepsilon2 + varepsilon1);
sun2 := M1(phi) = B*(mu*varkappa2 + varkappa1);
sun3 := N1 = (diff(A2*M1(phi), phi) - diff(A2, phi)*M2)/(A1*A2);
sun4 := diff(A2*T1(phi), phi) - diff(A2, phi)*T2 + (N1/R1 + q1)*A1*A2
- A1*A2*T1(phi)*vartheta(phi)/R1 = 0;
sun5 := diff(A2*N1, phi) - (T1(phi)/R1
+ T2/R2)*A1*A2 + qn*A1*A2
diff(-A2*T1(phi)*vartheta(phi), phi) = 0;
equs := sun1, sun2, sun3, sun4, sun5;
bc := u(-Pi/2) = 0, w(-Pi/2) = 0, vartheta(-Pi/2) = 0, T1(Pi) = F,
M1(Pi) = m, kappa*G*h*(vartheta(Pi) + D(w)(Pi)/A1 - u(Pi)/R1) = P;
sys := [bc, equs];
vars := [M1(phi), T1(phi), u(phi), w(phi), vartheta(phi)];
nonmd := dsolve(sys, vars, numeric, output = listprocedure);
M11[k] := rhs(nonmd[2]);
Q1[k] := kappa*G*h*(rhs(nonmd[5]) + rhs(nonmd[7])/A1 - rhs(nonmd[4])/R1);
N11[k] := rhs(nonmd[3]);
hori[k] := rhs(nonmd[4])*cos(phi) + rhs(nonmd[6])*sin(phi);
verti[k] := -rhs(nonmd[4])*sin(phi) + rhs(nonmd[6])*cos(phi);
ur[k] := rhs(nonmd[4]);
wr[k] := rhs(nonmd[6]);
psi[k] := rhs(nonmd[5]);
print(k);

```

end do;

plot([seq(M11[k](phi), k = 2 .. 4)], phi = -Pi/2 .. Pi,

legend = ["k=2", "k=3", "k=4"], linestyle = [3, 5, 1],

color = ["black", "red", "blue"], axes = boxed)

References

- [1] V. V. Novozhilov, The Theory of Thin Shell. Noordhoff, Groningen, 1959.
- [2] S. Timoshenko and S. Woinowsky-Krieger, Theory of Plates and Shells, McGraw-Hill, New York, 1959.
- [3] H. Kraus, Thin Elastic Shells. John Wiley and Son, New York, 1967.
- [4] C. R. Calladine, Theory of Shell Structures. Cambridge University Press, 1983.
- [5] W. Flügge, Stresses in Shells. Springer-Verlag Berlin, 1973.
- [6] A. Libai and J. Simmonds, 1998. The Nonlinear Theory of Elastic Shells. Cambridge University Press.
- [7] B. Audoly and Y. Pomeau, Elasticity and Geometry - From hair curls to the non-linear response of shells. University of Cambridge, Cambridge, 2010.
- [8] B.H. Sun, Closed-form solution of axisymmetric slender elastic toroidal shells, Journal of Engineering Mechanics, 136 (10) (2010)1281-1288.
- [9] B.H. Sun, Toroidal Shells. Nova Science, New York, 2012.
- [10] B.H. Sun, Small Symmetrical Deformation of Thin Torus with Circular Cross-Section. Thin-Walled Structures 163 (2021) 107680.
- [11] B.H. Sun, Geometry-induced rigidity in elastic torus from circular to oblique elliptic cross-section, Int.J. of Non-linear Mechanics 135 (2021) 103754.
- [12] A. Zingoni, Shell Structures in Civil and Mechanical Engineering. ICE Publishing, 2018.
- [13] H. Reissner, Spannungen in Kugelschalen (Kuppeln). Festschrift Heinrich Müller-Breslau, A. Kröner, Leipzig (1912)181-193.
- [14] E. Meissner, Das elastizitätsproblem dünner schalen. Phys.Zeitschr. 14(1913) 343–349.
- [15] E. Meissner, Über und Elastizität Festigkeit dünner Schalen, Viertelschr. D. nature.Ges., Bd.60 (1915) Zurich.
- [16] Wissler, H., Festigkeiberechnung von Ringsflächen, Promotionarbeit, Zurich, 1916.
- [17] F. Tölke, Zur integration der differentialgleichungen der drehsymmetrisch belasteten rotationsschale bei beliebiger wandstärke. Ingenieur-Archiv. 9((1938)) 282–288.
- [18] W. Chang, Derspannungszustand in kreisringschale und ähnlichenSchalen mit Scheitelkreisringen unter drehsymmetrischer Belastung, Arbeitzur Erlangung des Grades eines Doctor-Ingenieurs der Technichen Hochschule, Berlin, 1944.(published in Scitific Report of Nattional Tsinghua University, Ser A. 289-349, 1949.)
- [19] R. J. Zhang and W. Zhang, Toroidal shells under Nonsymmetric Loading, Int. J. Solids Structures, 31(19)(1994) 2735-2750.
- [20] L. N. Tao, On toroidal shells, J. of Math and Physics. 38(1959)130-134.
- [21] A. Ronveaux, Heun's Differential Equations, Oxford University Press, 1995.
- [22] R. D. Mindlin, Thickness-shear and flexural vibration of crystal plates. Journal of Applied Physics. 22(1951) 316–323
- [23] R.D. Mindlin, High frequency vibrations of crystal plates. Q. Appl. Math. 19, 51–61 (1961)

- [24] R. D. Mindlin, "An introduction to the mathematical theory of vibrations of elastic plates," edited by J. S. Yang, World Scientific , 23-34, New Jersey (2006)
- [25] J. N. Reddy, A simple higher-order theory for laminated composites plates. *Journal of Applied Mechanics*. 51(1984) 745–752.
- [26] J. N. Reddy, *Theory and Analysis of Elastic Plates and Shells*. CRC Press, 2007.
- [27] X. H. Wang and D. Redekop, Natural frequencies analysis of moderately-thick and thick toroidal shells. *Procedia Engineering*. 14(2011)636–640.
- [28] A.E.H. Love, *A Treatise on the Mathematical Theory of Elasticity* (3rd ed.). Cambridge University Press, 1902.
- [29] J.L.J. Sanders and A. Liepins, Toroidal membrane under internal pressure. *AIAA Journal*. 1(1969) 2105–2110.
- [30] Marple <https://www.maplesoft.com/>
- [31] H.S. Tzou, *Piezoelectric Shells* (Kluwer, Dordrecht, 1993)
- [32] J.S. Yang, *The Mechanics of Piezoelectric Structures* (World Scientific, Singapore, 2006)